Applied Clay Science 163 (2018) 108–118

Contents lists available at ScienceDirect

Applied Clay Science

journal homepage: www.elsevier.com/locate/clay

Research paper

The use of mineralogical indicators for the assessment of firing temperature in fired-clay bodies

Alberto Viani[a,*], Giuseppe Cultrone[b], Konstantinos Sotiriadis[a], Radek Ševčík[a], Petr Šašek[a]

[a] Institute of Theoretical and Applied Mechanics of the Czech Academy of Sciences, Centre of Excellence Telč, Batelovská 485, CZ- 58856 Telč, Czechia
[b] Department of Mineralogy and Petrology, Faculty of Sciences, University of Granada, Fuentenueva s/n, 18002 Granada, Spain

ARTICLE INFO

Keywords:
Fired-clay bricks
X-ray diffraction analysis
Rietveld method
Firing temperature
Amorphous fraction

ABSTRACT

Fired-clay bricks are frequently object of conservative actions aimed at the preservation of cultural heritage. Information on firing conditions is relevant for the production of custom made replacement bricks, since, as a widely accepted principle, they should be close match to the pre-existing ones. In this work, the mineralogical and microstructural evolution of fired-clay bodies is described using a combination of analytical techniques, and an approach for the assessment of firing temperature using calibration curves built from the results of X-ray powder diffraction quantitative phase analysis with the Rietveld method, is presented. The weight fractions of hematite, mullite and the amorphous fraction, from two raw clays fired in the laboratory at different temperatures, have been used to assess the firing temperature of two industrially produced bricks. The values derived applying these three methods were in good agreement with the nominal temperatures of the industrial cycles. This approach might be of interest for the assessment of the firing conditions of a broader range of historical/archaeological fired-clay materials.

1. Introduction

The use of fired-clay bricks as construction material spread throughout Europe under the influence of the Romans. Although with geographical differences, it continued later, it flourished during the 19th century, and declined towards the second half of the 20th century.

Many brickworks have become objects of cultural heritage, and, because exposed for long time to a range of different environmental conditions, are nowadays raising various conservation issues (Baer and Livingstone, 2015; de Rojas et al., 2004; Maniatis et al., 1981; Schiavon et al., 2008). The conservation principles, established at national and international level, recommend the use of materials or techniques which are close matches for those being repaired or replaced, because they are recognised to carry a low risk of future harm or premature failure (Scolforo and Browne, 1996). For example, in case of stone objects, it is advisable, and sometimes possible, to use material from the same geological formation, or even the same quarry. The information about the source material is usually retrieved combining historical, archaeological and archaeometric data. For the replacement of fired-clay bricks, it would be required to gain knowledge of both the production process and the employed raw clay. Between the process variables, the maximum firing temperature has been considered of primary interest, because of its influence on the microstructure and, in turn, on the mechanical properties and the susceptibility of bricks to deterioration (Bauluz et al., 2004; Cultrone et al., 2004, 2005; Elert et al., 2003). In a recent study of historical bricks it has been proposed that the weight fraction of hematite and the unit-cell parameter of Mg-spinel might be used as indicators of firing temperature (Viani et al., 2016). This is in agreement with previous experimental evidences about the mineralogical, physical and chemical modifications occurring in clay bodies during thermal treatment (Cultrone et al., 2004; Khalfaoui and Hajjaji, 2009; McConville and Lee, 2005).

During firing of raw clays for brick production, sintering and recrystallization of the product of decomposition of clay minerals and development of new silicate phases, result in a new mineral assemblage and the formation of a fraction of glassy/amorphous phase. A substantial contribution to the amount of hematite detected in bricks comes from the iron initially present in the phyllosilicates of the raw clay (De Bonis et al., 2017), whereas Mg-spinel mostly forms as decomposition product of clinochlore (Barlow et al., 1997; Khalfaoui et al., 2006; Khalfaoui and Hajjaji, 2009), illite and kaolinite (McConville and Lee, 2005). Therefore, the firing conditions and the nature of the raw clay define the mineralogy and microstructure of the fired body (Cultrone et al., 2004). For example, relatively high spinel content (2.6–5.3 wt%) has been related to the chloritic nature of the clay feeding material (Viani et al., 2016). The unit-cell parameter of

* Corresponding author.
E-mail address: viani@itam.cas.cz (A. Viani).

https://doi.org/10.1016/j.clay.2018.07.020
Received 21 May 2018; Received in revised form 11 July 2018; Accepted 13 July 2018

spinel was considered a potential indicator of firing temperature, because essentially dependent upon the content in foreign ions, which increases with temperature, and less on the chemical composition of the raw clay.

The soundness of this, as well as of other methods, necessarily rests on an empirical basis, because of the complexity of the system and the process variables involved. It is therefore essential to extend the knowledge of the mineralogical and microstructural evolution of fired bodies to a larger number of raw clay materials. To this aim, and in order to contribute in the definition of a methodology based on mineralogical and/or microstructural parameters for the assessment of the firing conditions in fired-clay bricks, in this work raw clays from two brickyards of Czech Republic have been fired in a range of temperatures and dwell times. The raw clays and the fired products have been characterized with a combination of analytical techniques, and correlation curves for some mineralogical parameters, have been built. Results have been compared with those obtained from bricks fired in the production cycles of the two brickyards.

2. Materials and methods

In this study the raw clay and production bricks were collected from two localities in Czech Republic, namely, Štěrboholy and Sedlejov.

2.1. Site description and geological context

The brickyard located in Štěrboholy, now within the metropolitan area of Prague, started operation in 1927, but brick production in this area is much older. The original circular kiln has been substituted in 1992 with a tunnel kiln. Custom-sized bricks from this plant have been employed as replacement bricks for conservation works in Austro-Hungarian historical fortresses of the late 18th century, now located in Czech Republic, namely, Josefov and Terezin (Slavík et al., 2014). The raw clays are obtained from the nearby deposits. Nowadays, after excavation, they are homogenized and stockpiled at least for one year before use. Size reduction (< 5 mm) is followed by tempering and extrusion. The bricks are then dried at 80 °C for 6 days and later introduced in the kiln. According to the brick type, different firing cycles are in use. For the sample used in this study, the cycle comprised preheating at 140 °C, firing at nominal temperature between 950 °C and 1000 °C and cooling, lasting in complex 2 days.

The Štěrboholy area is part of Úvaly platform (part of bigger Říčany platform). The rock basement is formed mostly by Paleozoic rocks and relics of Mesozoic and Quaternary sediments (Chlupáč et al., 2002). The most common rock types are Paleozoic (upper Ordovician) dark grey/black, clay-rich and fine grained shales with organic content < 1% which contain some pyrite and gypsum. Other frequently represented rocks are fine grained siltstones (upper Ordovician) with calcite concretions. Other relics of the Ordovician strata are mostly black shales with higher organic content. The Quaternary sediments (Paleogene and Neogene), mostly of eluvial and fluvial origin, related to the erosion of the older rocks, are fine grained calcitic and clay-rich siltstones used as raw material in brick manufacturing (Kovanda et al., 2001).

The brickyard once located near the village of Sedlejov, few km from the historic town of Telč (Vysočina region), started production in 1922 and ended in 1972. It was equipped with a Hoffmann kiln with rooms for firing brick pallets in sequence, while maintaining the fire burning (Akinshipe and Kornelius, 2017). The excavated raw clay, was stockpiled before use and the extruded bricks were fired at temperature between 950 °C and 1000 °C (personal communication). Further details of the firing cycle were not available to the authors.

The geology of the Telč area is dominated by granitic rocks of the Moldanubicum massif (Luna, 2005). The latter is a Precambrian unit which underwent several metamorphic episodes. The rocks are mainly paragneiss and granites. Around Telč, the composition is rather homogeneous, consisting of small-to medium-grained mica monzogranites to granites with a predominance of quartz, potassium feldspar, plagioclase, biotite and muscovite. The superficial deposits are only tiny Neogene remnants and Quaternary products of weathering of the surrounding rocks. They include loess and loess loams, together with sandy and loamy fluvial sediments. The raw clays used in brick manufacturing were excavated from these Quaternary deposits. Geological maps at the scale 1:50000 of both areas are accessible through the website of the Czech Geological Survey (ČGS, 2018).

2.2. Materials

Dried extruded bricks from Štěrboholy brickyard have been used in the firing experiments conducted at the laboratory scale. 4 cm-edge cubes were cut from them before firing. In case of the brickyard of Sedlejov, since it no more exists, about 20 kg of raw clay were obtained from the original pit (coordinates: 50°04′49.9″N 14°32′41.6″E) several months after the material was exposed by an excavator. The raw clay was homogenized and reduced in size below 5 mm. The optimal conditions for laboratory screw extrusion through a die 4 × 4 cm resulted in 20.6 wt% of water added. 4 cm-edge cubes were obtained. The samples were kept in oven at 50 °C for 24 h and then at 80 °C for 24 h before firing. Firing was carried out in an electrical laboratory furnace under oxidizing conditions. The samples were preheated at 100 °C for 1 h and then brought to maximum temperature at heating rate 3 °C/min. Dwell times of 3 h were used. The samples were left to cool down by switching off the furnace. The following maximum firing temperatures were reached: 800 °C, 900 °C, 950 °C, 1000 °C, 1050 °C and 1100 °C. Additional dwell times of 5, 7 and 12 h at maximum firing temperature of 950 °C were also tested. One brick fired in the industrial cycle was collected from both sites. Samples were named using SE and ST for Sedlejov and Štěrboholy areas, respectively, followed by a number corresponding to the firing temperature in °C, or the letter B, to indicate the brick fired in the brickyard.

2.3. Analytical methods

Chemical analysis of the raw clays have been accomplished with X-ray fluorescence method using pressed pellets of finely ground samples dried at 110 °C overnight. Loss on ignition was measured after firing at 1100 °C.

The textural and microstructural features of the bricks were observed in thin section under a Carl Zeiss Jenapol-U polarized optical microscope (POM) equipped with digital photocamera. The sections were cut with orientation perpendicularly to the direction of extrusion. Investigations with field emission scanning electron microscope (FESEM) were performed on the same thin sections used for POM, but carbon coated. A Carl Zeiss SMT AURIGA instrument equipped with an energy dispersive detector AZTEC (Oxford Instruments) was used. The samples were coated with 5 nm thick gold film prior to analysis and observed at 20 kV accelerating voltage.

MIP analysis for pore-size distribution, bulk density, skeletal density and total porosity was conducted in triplicate on fragments cut from the central part of each sample. A Micrometrics AutoPore IV 9500 porosimeter, working at maximum pressure of 228 MPa, was employed. The covered range in pore diameter was 0.006–376 μm.

X-ray powder diffraction (XRPD) was performed for quantitative phase analysis (QPA) of both fired bodies and raw clays, previously dried at 110 °C overnight and then ground and homogenized by hand in agate mortar. Data were collected in the angular range 4–82° 2θ with virtual step scan of 0.0102° 2θ and 0.4 s/step counting time, by using Cu radiation at 40 kV and 40 mA. The Bragg–Brentano θ-θ diffractometer (Bruker D8 Advance pro) was equipped with a LynxEye 1-D silicon strip detector. Divergence 0.6 mm slit and 2.5° Soller slits were mounted on the incident beam pathway, whereas Ni filter, to select the K_α line (λ = 1.5418 Å), and Soller slits (2.5°) were mounted on the diffracted beam pathway. The samples were allowed to spin at 15 rpm

to improve particle statistics. The side loading technique was used in order to minimize a priori preferred orientation of crystallites. QPA was performed on bricks and raw materials with the Rietveld method. Both crystalline and amorphous fractions were quantified for fired samples by spiking them with 10 wt% of internal standard α-Al_2O_3 (NIST SRM 676a) (Cline et al., 2011). The accuracy of this approach has been already tested on natural raw materials and industrial products, including bricks and ceramics (Gualtieri et al., 2004, 2014; Gualtieri and Brignoli, 2004). Refinements were performed with the TOPAS 4.2 software (Bruker AXS) employing the fundamental parameter approach.

3. Results

3.1. Microscopy

A selection of images collected from POM and FESEM is presented in Figs. 1 and 2, respectively. Microstructure of fired samples will be described from a qualitative standpoint, as usually reported in the literature. Under the microscope, the two groups of samples fired in the laboratory appear different from the textural point of view. ST and SE samples are mainly composed of quartz and feldspar grains, constituting the temper of the fired body, dispersed in a matrix more or less vitrified, depending on the firing temperature. The size and morphology of these grains, as well as the degree of cohesion between grains and matrix, the pore shape and distribution, differ.

Under POM, in the ST samples, grains are up to 5 mm in size, composed of quartz and rock fragments very rich in Fe oxides (Fig. 1a). Less frequently, anhydrite grains, feldspars and plagioclase with albite twinning, have been identified. The matrix is composed of small and partially oriented phyllosilicates crystals with yellow interference color. Starting form 950 °C, the matrix shows less birefringence. At 1000 °C and 1100 °C the texture appears more compact (Fig. 1b). The SE sample fired at 800 °C exhibits high birefringence and the temper, finer compared to ST samples (up to 200 μm), is mainly composed of quartz grains with mosaic texture and undulated extinction, which suggest their metamorphic origin, and less abundant plagioclase and feldspar grains (Fig. 1c). The matrix loses its birefringence at 1000 °C (i.e., 50 °C higher than ST samples). No differences can be observed at 1100 °C (Fig. 1d).

FESEM observations reveal that at 800 °C in ST samples no reaction has occurred. As shown in Fig. 2a, since the sections were cut perpendicularly to the direction of extrusion, elongated grains and phyllosilicates show preferred orientation. Phyllosilicates preserved their original morphology, although a slight separation along their 001 planes, because of dehydroxylation (loss of OH^-) was observed. Occasionally, small bright grains of ilmenite, scattered monazite and apatite crystals and hornblende-like amphibole fragments with double exfoliation system, have been identified. Some grains of temper are very rich in hematite. They exhibit skeletal morphology and, in some cases, resembling the framboidal pyrite structure, which may be considered an indication of their origin (anoxic environment). At 900 °C, the separation of the phyllosilicate sheets, increases. Fig. 2b illustrates hematite crystal showing the hexagonal habit and growth zoning. This may suggest a topotactic replacement of a Fe-hydroxide phase, like lepidocrocite, identified in the raw clay by XRPD, that upon dehydroxylation converted into maghemite and then to the most stable hematite (de Bakker et al., 1991). Hematite crystals have been also identified at higher temperature with the same morphology. At 950 °C, a secondary porosity inside exfoliated phyllosilicate starts to develop. Rare reaction rims surrounding silicates (i.e., quartz and micas) were observed. Some grains of anhydrite have been also identified by EDX analysis (Fig. 2c). In this case, it can be noted that the crystal edges are not in contact with the matrix, because of the dehydration of the former hydrated Ca sulphate (gypsum or bassanite), which caused substantial volume contraction. At 1000 °C phyllosilicates are losing their laminar morphology and the development of secondary porosity is more evident. At 1100 °C samples are totally vitrified and phyllosilicates are no longer recognizable. Rounded or elongated bubbles are frequent (Fig. 2d).

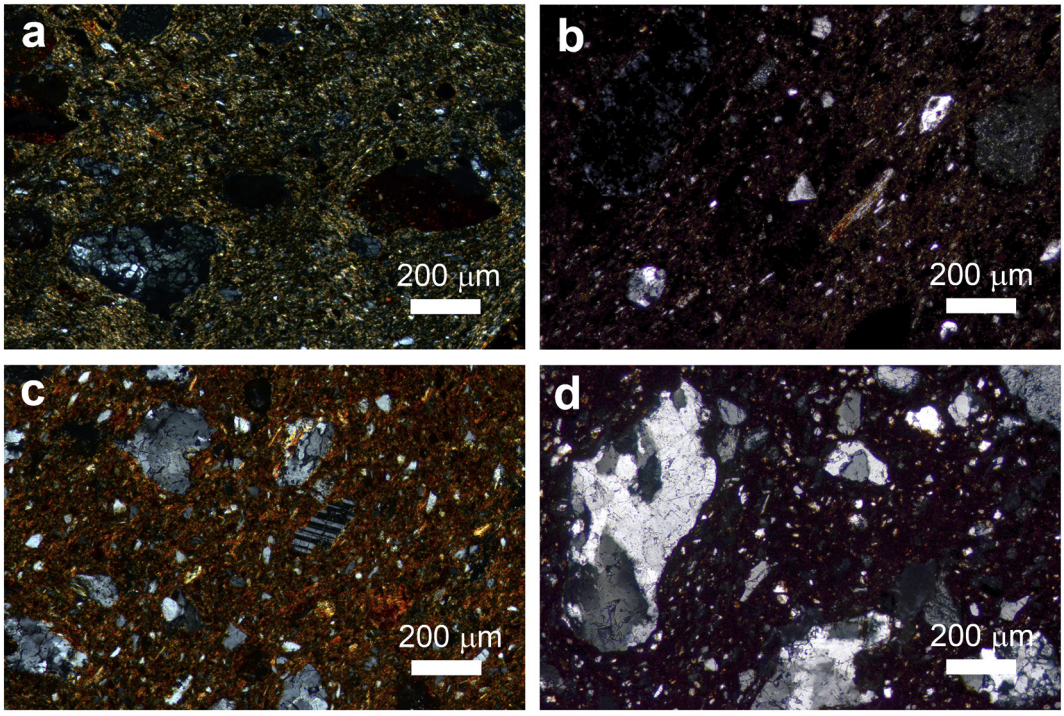

Fig. 1. Gallery of optical microscope images in cross-polarized light in thin section. a) general view of sample ST800. Elongated Fe-oxide grains (red-orange) with smoothed edges and highly fractured anhydrite grains (light grey), are visible; b) low birefringence of sample ST1100 in which only quartz grains can be easily recognised. Note the preferred orientation of elongated grains (maybe former phyllosilicates); c) angular quartz grains and plagioclase with albite twinning in a reddish matrix in SE800 sample; d) image of SE1000 characterized by low birefringence in which quartz fragments with mosaic texture can be identified.

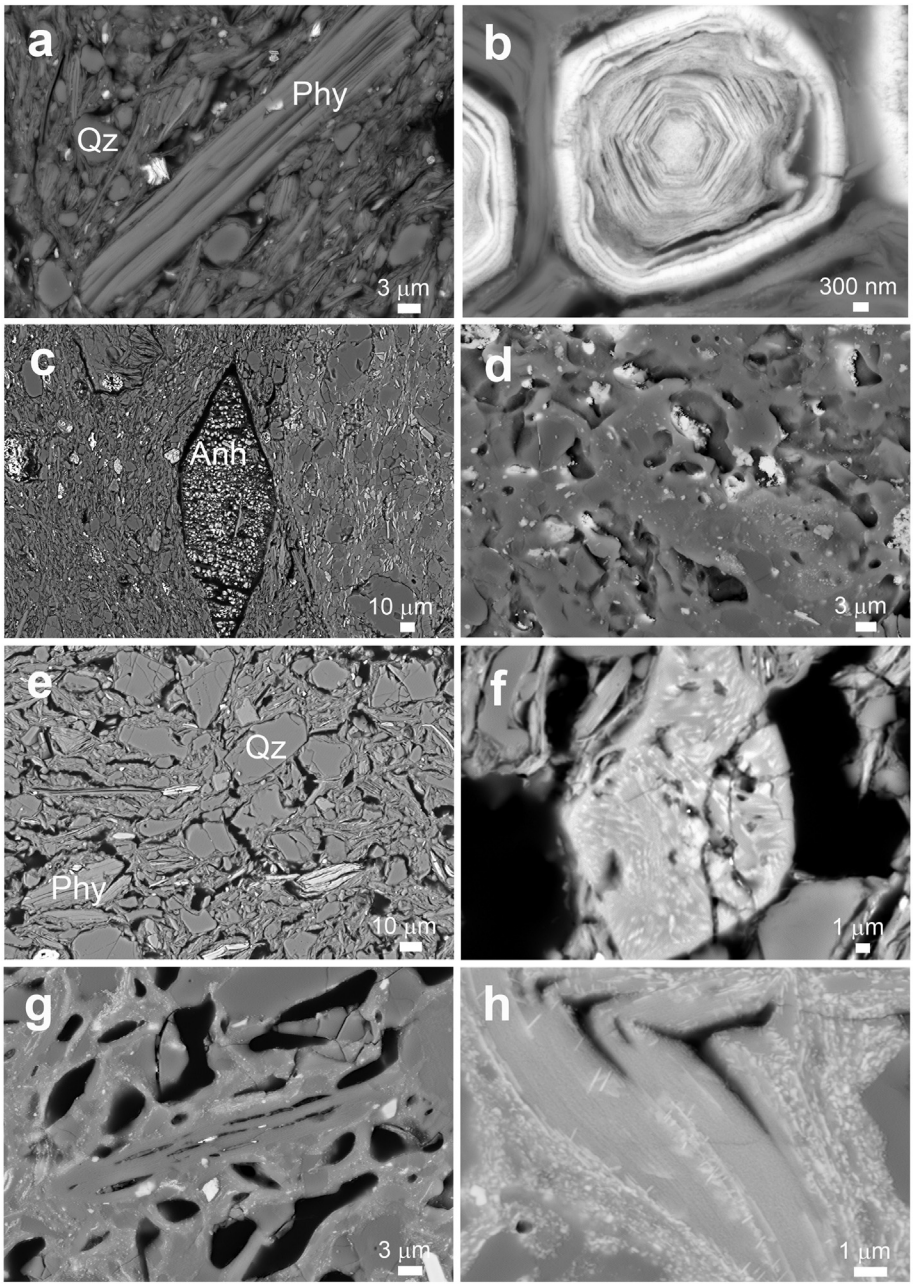

Fig. 2. Gallery of HRSEM micrographs of some of the investigated samples. a) preferred orientation of elongated crystals in ST sample fired at 800 °C; b) detailed image of hematite crystal with hexagonal shape and growth zoning in ST900; c) highly fractured anhydrite crystal in ST950; d) totally vitrified matrix with the development of rounded bubbles in ST1100; e) general view of the texture of SE sample fired at 800 °C; f) development of micrometric and submicrometric brighter gehlenite crystals in SE950; g) high vitrified SE ceramic fired at 1100 °C in which former phyllosilicate is still recognizable; h) Fe-rich oxides (i.e., hematite) growth along phyllosilicate sheets in SE1100. Legend: Qz = quartz; Phy = phyllosilicate; Anh = anhydrite.

As regard SE samples, at 800 °C one can observe a poorest link among grains if compared to ST samples fired at the same temperature (Fig. 2e). Quartz and phyllosilicates are by far the most abundant phases, some grains of hornblende, anorthitic plagioclase and small fragments of ilmenite have been observed and identified by EDX analysis. The dehydroxylation of phyllosilicates is more evident at 900 °C, and at 950 °C, a secondary porosity, with the presence of small bubbles starts to develop, together with rare reaction rims surrounding silicates (Fig. 2f). The vitrification grows at 1000 °C and reaches a maximum at 1100 °C with the formation of rounded pores. The link among grains improved significantly. However, at the highest firing temperature the laminar habit of phyllosilicates is sometimes still visible (Fig. 2g). An enrichment in Fe along phyllosilicates sheets with the growth of small hematite crystals, has been detected (Fig. 2h).

Both SEB and STB samples, from bricks fired in the industrial cycle, exhibited textural features and mineralogical assemblages observed in the corresponding samples fired in laboratory between 950 °C and 1000 °C. Typically, phyllosilicates show preferred orientation, due to the extrusion process, and exfoliation, with development of secondary porosity, resulting by partial decomposition. The vitrification is not much developed in both samples, pointing to temperatures not exceeding 1050 °C.

3.2. MIP porosity

Bulk and skeletal density and open porosity obtained from MIP, are reported in Table 1. Porometric distribution is available in Fig. 3. The bulk density values increased with firing temperature for the samples prepared in the laboratory, as a consequence of the densification process accompanying firing (Delbrouck et al., 1993).

Compared to them, the value measured for the brick from Štěrboholy fired in the industrial kiln, indicates a temperature around 1000 °C, whereas the bulk density of the corresponding brick from Sedlejov points to lower values, around 800–900 °C. The skeletal density increases up to 1000 °C, to decrease above. This is reflecting the development of close porosity at high temperature, inaccessible to the

Table 1
Bulk density (ρ_b), skeletal density (ρ_s) and MIP porosity, average values from studied samples. Where not reported, standard deviation is below 1%.

Sample	ρ_b (g/cm^3)	ρ_s (g/cm^3)	Porosity (%)
SE800	1.80	2.52	28.5 (0.4)
SE900	1.82	2.59	29.7 (0.2)
SE950	1.83	2.58	29.0 (0.2)
SE1000	1.88	2.56	26.6 (0.6)
SE1050	1.99	2.53	21.2 (0.3)
SE1100	2.09	2.48	15.6 (0.9)
SEB	1.81	2.52	28.0 (0.1)
ST800	1.76	2.54	30.8 (0.2)
ST900	1.86	2.64	29.7 (0.9)
ST950	1.93	2.62	26.2 (1.4)
ST1000	2.09	2.65	21.1 (1.1)
ST1050	2.28	2.51	9.2 (1.5)
ST1100	2.31	2.45	5.6 (0.7)
STB	2.01	2.69	25.3 (0.5)

probing fluid. The industrial brick from Sedlejov exhibits the lowest value, whereas the brick from Štěrboholy the highest.

For the samples fired in the laboratory, the maximum in the curve of differential intruded volume vs. pore diameter shifts towards larger pores as the firing temperature increases, whereas the MIP porosity decreases. This has been already explained in terms of progressive vitrification of bricks with the development of rounded pores due to gas escape and at the same time the reduction of pore connectivity when raw clays are fired above 900 °C (Cultrone et al., 2004; Delbrouck et al., 1993; Freyburg and Schwarz, 2007).

3.3. QPA results

Results from the QPA of the samples fired at increasing temperatures and raw materials are reported in Tables 2 and 3. Agreement factor R_{wp} of the refinements, as defined in TOPAS (Young, 1993), ranged between 4.6 and 6.5. An example of graphical output of Rietveld refinement for sample SE900 and the raw clays are provided as Supplementary material Figs. S1 and S2, respectively.

In the raw clay from Sedlejov, illite/muscovite and kaolinite comprised > 30 wt%, whereas, clinochlore and montmorillonite sum up to about 15 wt%. The raw clay from Štěrboholy showed a higher content of illite/muscovite (38.1 wt%), a small weight fraction of mixed layer clay minerals and no montmorillonite. The mineralogical composition reflects the nature of their respective geological districts, since the raw clay deposits are recent geological units (Quaternary) which formed from the weathering of the surrounding rocks (Kovanda et al., 2001; Luna, 2005). Accordingly, SE raw clay has a higher amount of quartz and a higher content in albite in the feldspars, together with a high content of muscovite compared to ST, because of the granitic nature of the rocks of the Telč area.

Despite the literature reports mostly of raw clays for brick

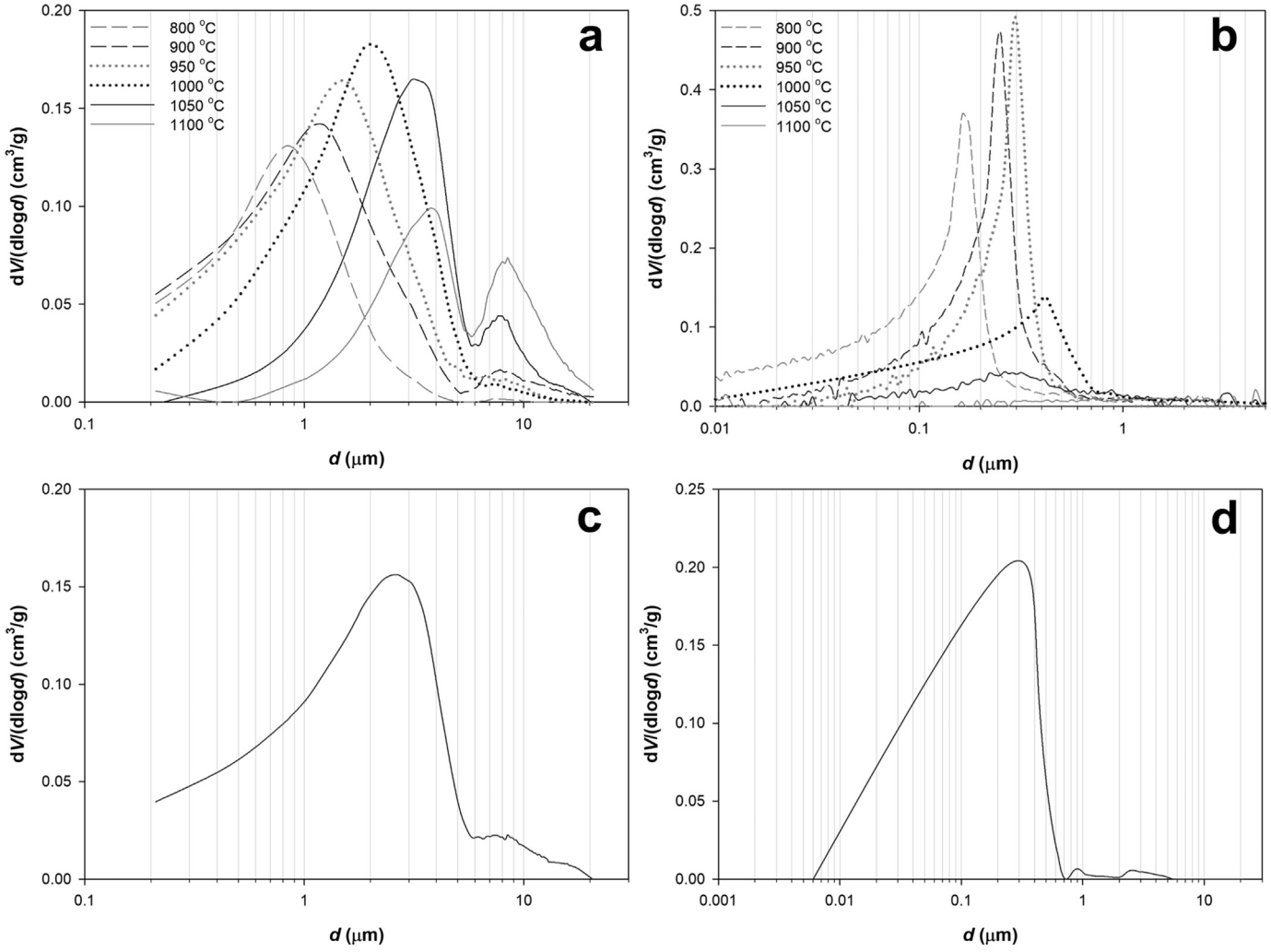

Fig. 3. MIP pore-size distribution curves of Sedlejov (a) and Štěrboholy (b) raw clays fired in laboratory, and Sedlejov (c) and Štěrboholy (d) bricks of industrial production.

Table 2
Quantitative phase analysis (wt%) of samples fired in the laboratory, industrial brick (SEB) and raw clay from Sedlejov as determined by Rietveld refinement of XRPD data. Standard deviations from the refinement are reported.

Phase	Sample						SEB	Raw clay
	SE800	SE900	SE950	SE1000	SE1050	SE1100		SE
Q	44.0 (0.3)	47.7 (0.2)	45.5 (0.2)	42.2 (0.2)	39.0 (0.2)	36.5 (0.2)	40.6 (0.2)	39.8 (0.1)
Spl	–	–	–	2.1 (0.1)	2.2 (0.1)	2.2 (0.1)	–	–
Kfs	5.3 (0.2)	4.3 (0.2)	5.0 (0.1)	4.6 (0.1)	2.7 (0.1)	0.9 (0.1)	4.8 (0.1)	4.6 (0.3)
Ab	4.7 (0.3)	4.3 (0.2)	2.9 (0.2)	3.5 (0.2)	2.6 (0.2)	1.7 (0.1)	3.8 (0.1)	4.6 (0.3)
An	2.8 (0.2)	1.9 (0.2)	1.7 (0.2)	1.2 (0.2)	1.8 (0.2)	1.7 (0.2)	2.2 (0.2)	2.0 (0.2)
I/Ms	11.7 (0.2)	10.2 (0.2)	3.7 (0.1)	–	–	–	5.0 (0.2)	17.4 (0.5)
Hem	0.7 (0.1)	1.3 (0.1)	2.0 (0.1)	2.4 (0.1)	2.9 (0.1)	3.2 (0.1)	2.1 (0.1)	–
Amp	0.8 (0.1)	–	0.5 (0.1)	–	–	–	0.3 (0.1)	1.1 (0.2)
Mul	–	–	1.2 (0.1)	1.8 (0.1)	3.3 (0.1)	6.0 (0.1)	1.5 (0.1)	–
Kaol	–	–	–	–	–	–	–	16.6 (0.4)
Clc	–	–	–	–	–	–	–	7.4 (0.5)
Mt	–	–	–	–	–	–	–	6.4 (0.4)
Am	30.0 (0.9)	30.2 (0.9)	38 (1)	42.3 (0.8)	45.4 (0.8)	47.5 (0.7)	39.6 (0.7)	–

Q = quartz; Spl = spinel; Kfs = K-feldspar; Ab = albite; An = anorthite; I/Ms. = illite/muscovite; Hem = hematite; Amp = amphibole; Mul = mullite; Kaol = kaolinite; Clc = clinochlore; Mt. = montmorillonite; Am = amorphous phase.

Table 3
Quantitative phase analysis (wt%) of samples fired in the laboratory, industrial brick (STB) and raw clay from Štěrboholy, as determined by Rietveld refinement of XRPD data. Standard deviations from the refinement are reported.

Phase	Sample						STB	Raw clay
	ST800	ST900	ST950	ST1000	ST1050	ST1100		ST
Q	28.9 (0.2)	29.4 (0.2)	28.2 (0.3)	28.8 (0.3)	26.4 (0.2)	18.8 (0.2)	26.8 (0.2)	34.4 (0.1)
Spl	–	1.0 (0.1)	2.1 (0.1)	3.3 (0.1)	2.7 (0.1)	2.0 (0.1)	2.0 (0.1)	–
Kfs	3.8 (0.2)	< 0.5	< 0.5	–	–	–	–	2.4 (0.2)
Ab	1.6 (0.2)	< 0.5	0.8 (0.1)	< 0.5	–	< 0.5	0.8 (0.1)	–
I/Ms	22.0 (0.3)	10.8 (0.2)	4.5 (0.2)	–	–	–	2.7 (0.2)	38.1 (0.4)
Hem	3.4 (0.1)	4.2 (0.1)	4.4 (0.1)	4.9 (0.1)	5.1 (0.1)	5.6 (0.1)	4.7 (0.1)	1.3 (0.1)
Anh	0.6 (0.1)	0.8 (0.1)	1.0 (0.1)	< 0.5	–	0.9 (0.1)	1.2 (0.1)	–
Amp	–	–	–	–	–	–	–	–
Mul	–	1.6 (0.1)	2.1 (0.1)	3.6 (0.2)	6.2 (0.2)	12.0 (0.2)	3.2 (0.1)	–
Kaol	–	–	–	–	–	–	–	17.6 (0.3)
Clc	–	–	–	–	–	–	–	2.3 (0.1)
I-Sm	–	–	–	–	–	–	–	2.2 (0.1)
Lep	–	–	–	–	–	–	–	1.1 (0.1)
Bas	–	–	–	–	–	–	–	< 0.5
Am	40 (1)	51.5 (0.7)	56.7 (0.7)	58.7 (0.8)	59.6 (0.8)	60.4 (0.6)	58.6 (0.6)	–

Q = quartz; Spl = spinel; Kfs = K-feldspar; Ab = albite; I/Ms. = illite/muscovite; Hem = hematite; Anh = anhydrite; Amp = amphibole; Mul = mullite; Kaol = kaolinite; Clc = clinochlore; I-Sm = illite/smectite; Lep = lepidocrocite; Bas = bassanite; Am = amorphous phase.

manufacturing containing carbonates (Cultrone et al., 2005; De Rosa and Cultrone, 2014; Dondi et al., 2004; Elert et al., 2003; Gualtieri et al., 2010; Podoba et al., 2014), in the present case, both raw materials are deprived of carbonates.

The results of chemical analysis, reported in Table 4, are, in general, in good agreement with the QPA, although most of the minerals show a complex pattern of isomorphic substitutions which do not allow for extracting accurate chemical composition from mineralogical analysis. From a qualitative standpoint it can be inferred that the raw clay from Sedlejov is richer in SiO_2 and poorer in K_2O likely because of its higher quartz content and lower content in illite/muscovite. The detected sulfur in the raw clay from Štěrboholy must be related to the presence of calcium sulphate, in agreement with QPA and geological information. Less straightforward is the justification of the other detected differences between the two raw clays.

Table 4
Chemical analysis of the raw materials employed as determined by X-ray fluorescence and measured loss on ignition (L.O.I.). Values are in wt%.

Oxides	Chemical composition	
	SE	ST
SiO_2	63.5	61.2
Al_2O_3	19.1	18.7
Fe_2O3	2.9	5.4
CaO	2.7	1.2
MgO	1.6	2.9
Na_2O	1.0	1.0.
K_2O	1.7	3.1
TiO_2	0.3	0.9
MnO	0.2	–
SO_3	–	0.5
L.O.I.	7.1	5.2

In the fired samples, quartz and amorphous fraction are the most abundant phases, in agreement with results of similar experiments in which the amorphous fraction has been quantified (Alonso-Santurde et al., 2011; Ballato et al., 2005; Freyburg and Schwarz, 2007; Gualtieri et al., 2014; Viani et al., 2016). The weight fraction of quartz does not show a monotonic trend with firing temperature. Conversely, the amount of amorphous fraction correlates positively with firing temperature, in agreement with previous observations (Cultrone et al., 2004; Delbrouck et al., 1993). Illite/muscovite is detected up to 950 °C, whereas other minor minerals include Mg-spinel, hematite and feldspars. A small amount of anhydrite (below 1 wt%) in ST samples is due to the presence of bassanite in the raw clay. Mullite appears between

Table 5
Quantitative phase analysis (wt%) determined by Rietveld refinement of XRPD data of samples fired in the laboratory at max temperature of 950 °C increasing dwell time. Standard deviations from the refinement are reported.

Phase	Sample					
	SE950_5h	SE950_7h	SE950_12h	ST950_5h	ST950_7h	ST950_12h
Q	43.1 (3)	46.2 (2)	45.1 (2)	26.7 (2)	28.2 (2)	27.9 (2)
Spl	–	–	–	2.6 (1)	2.5 (1)	2.5 (1)
Kfs	4.8 (2)	5.7 (2)	5.8 (1)	–	–	–
Ab	3.8 (3)	3.3 (2)	4.0 (2)	1.2 (1)	0.6 (1)	0.8 (1)
An	1.9 (2)	1.5 (2)	1.7 (2)	–	–	–
I/Ms	3.4 (2)	2.9 (2)	2.8 (1)	2.7 (2)	2.5 (2)	2.8 (2)
Hem	2.1 (1)	2.0 (1)	2.2 (1)	4.7 (1)	4.6 (1)	4.8 (1)
Amp	0.3 (1)	0.5 (1)	0.8 (1)	–	–	–
Mul	1.3 (1)	1.2 (1)	1.6 (1)	2.4 (1)	2.9 (1)	2.9 (1)
Anh	–	–	–	0.6 (1)	1.0 (1)	< 0.5
Am	39.3 (0.9)	37.1 (9)	36.1 (9)	59 (1)	57 (1)	58 (1)

Q = quartz; Spl = spinel; Kfs = K-feldspar; Ab = albite; An = anorthite; I/Ms = illite/muscovite; Hem = hematite; Amp = amphibole; Mul = mullite; Anh = anhydrite; Am = amorphous phase.

900 °C and 950 °C and its content increases with firing temperature. Hematite content is also increasing with firing temperature.

In both series of samples fired in the laboratory at 950 °C, the increase in dwell time brings about a decrease in illite/muscovite and a limited increase of mullite and K-feldspar, the latter only for the samples SE (see Table 5). More erratic, and often within the standard error of the refinement, are the other variations. Relevant plots extracted from the reported tables will be discussed later.

4. Discussion

Both the microstructural and mineralogical information have a great potential for the characterization of bricks firing conditions. Since the latter directly reflects the sequence of reactions taking place during firing (Bauluz et al., 2004; Cultrone et al., 2001; Gualtieri, 2007; Viani et al., 2016), it has been considered in this respect more attractive. In practice, because of the different raw clay typologies and their complex mineralogical composition, the thermodynamic equilibria shift, and the kinetics of the transformation reactions are modified, hampering the identification of a mineralogical parameter common to a wide range of fired bodies. For example, in the present case, the association of Ca and Ca−Mg silicates, forming from the decomposition of carbonates during firing (Bauluz et al., 2004; Válek et al., 2014) was not observed because the raw clays are essentially deprived of carbonates, and the first reactions of which we have clear evidence from the QPA are those of dehydroxylation of phyllosilicates. As it should be expected, montmorillonite, illite/smectite, kaolinite and chlorite were not detected in none of the samples fired above 800 °C. The role of the above mentioned kinetic and compositional factors is apparent in the persistence of muscovite up to 950 °C (Cultrone et al., 2001; Rodriguez-Navarro et al., 2003). Its content decreases increasing dwell time up to 5 h in both SE and ST samples, whereas it is relatively constant for longer dwell times, up to 12 h.

The content in feldspars is more difficult to interpret because they are involved in the polymorphic transformation at high temperature, or form after phyllosilicate decomposition (Cultrone et al., 2001), making them less useful indicators of firing temperature (Khalfaoui and Hajjaji, 2009; Viani et al., 2016). The content in quartz exhibits a dependence from firing temperature and mineralogical composition of the raw clay. In sample SE, quartz content increases up to 900 °C, to decrease above this temperature. This might be in agreement with what reported for kaolinitic and illitic-kaolinitic clays (Freyburg and Schwarz, 2007; Laita and Bauluz, 2018), and be, at least in part, an indirect consequence of the water loss occurring during dehydroxylation of silicates. Formation of quartz from the breakdown of chlorite, as already proposed for the thermal decomposition of chloritic-illitic clays (Khalfaoui and Hajjaji, 2009), does not find confirmation here. The later decrease in quartz content is related to the reactions taking place at high temperature. Above 1000 °C, thanks to the fluxing role of alkaline feldspars, a silica-rich melt forms; quartz is partially decomposed, and secondary mullite crystallizes (Gualtieri, 2007; Iqbal and Lee, 2000). As a matter of fact, mullite is detected at 950 °C (1.2 wt%) and increases to 6.0 wt% at 1100 °C; in the same temperature interval the feldspar content decreases from 9.6 wt% to 4.3 wt%.

In sample ST, the trend is less clear and oscillatory until 1000 °C, more similar to what observed in firing clays enriched in three-layer minerals (Freyburg and Schwarz, 2007). In complex, from 900 °C to 1100 °C, the decrease in quartz content is much higher with respect to sample SE (36% against 23.5%). The content of illite/muscovite in the raw clay is almost two times higher, which promoted melt formation as early as 900 °C (Rodriguez-Navarro et al., 2003), as reflected in the steady increase in amorphous fraction (from 51.5 wt% to 60.4 wt%). These examples highlight the difficulties of deriving the firing conditions using as indicators residual phases (Bauluz et al., 2004; Podoba et al., 2014; Viani et al., 2016).

Conversely, some of the newly formed phases show a monotonic increase with firing temperature. When the content in hematite is plotted against firing temperature, as in Fig. 4, a linear positive correlation is observed in both SE and ST series of samples fired in the laboratory. This linear correlation can be used as a calibration curve, and its correctness verified deriving a firing temperature for the industrial bricks according to their content in hematite. The obtained values are 967 °C and 980 °C, for SEB and STB samples, respectively, which can be considered in good agreement with the available information about the firing cycles.

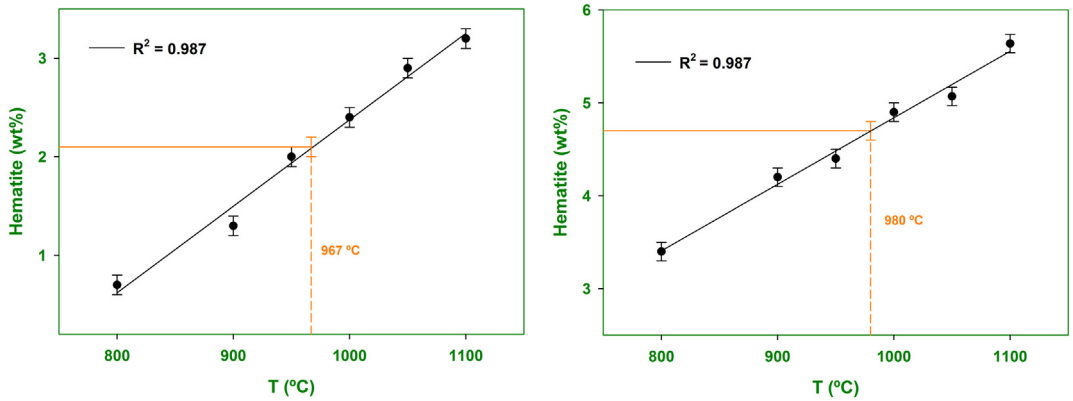

Fig. 4. Plot of hematite content vs. temperature with regression lines through the points for SE (left) and ST (right) samples fired in laboratory. Temperatures corresponding to bricks of industrial production are indicated.

A dependence from firing temperature of the amount of hematite has been already observed (Cultrone et al., 2004; Freyburg and Schwarz, 2007; Khalfaoui and Hajjaji, 2009; McConville and Lee, 2005; Maniatis et al., 1981), whereas a linear correlation in the temperature interval of relevance for brick manufacturing, was conjectured in a recent study of old bricks produced from chloritic clays (Viani et al., 2016). Here, it is for the first time exploited to derive the bricks firing temperature.

However, this approach may also hide pitfalls. First of all, the reported increase of weight fraction of hematite increasing dwell time (Cultrone et al., 2004; Khalfaoui and Hajjaji, 2009; McConville and Lee, 2005) must be considered. Unfortunately, quantitative data from the literature are scarce and highly scattered. Most of the reported datasets actually do not evidence an increase in hematite for dwell times > 2 h and < 15 h (Khalfaoui and Hajjaji, 2009; Valanciene et al., 2010). In the present investigation, essentially no increase in hematite for sample SE, has been observed, in agreement with the limited decrease in illite/muscovite, the main source of iron at this temperatures. On the contrary, an increase, mostly concentrated between 3 and 5 h, is observed for sample ST. This is likely connected with the partial decomposition of illite/muscovite, which decreases to the same content detected in sample SE. Basically, the higher the content in residual phyllosilicates, the higher the effect of dwell time on the amount of hematite which forms at the same temperature. It must be emphasized that, because the set of reactions taking place during the mineralogical evolution of the fired body depends on the nature of the raw clay, the application of the observed linear correlation to bricks obtained from raw clays with different mineralogical composition, must be experimentally verified. In case of raw clays containing carbonates, for example, a fraction of iron is subtracted and incorporated into some of the newly formed phases (e.g. clinopyroxene) (Bauluz et al., 2004; Valanciene et al., 2010).

Mullite and spinel, forming during brick firing, are also of interest as potential indicators of firing conditions. The significant amount of mullite, especially in samples fired above 950 °C, confirms it was one of the main products developed after illite/muscovite breakdown (De Rosa and Cultrone, 2014; Rodriguez-Navarro et al., 2003). However, the increase in mullite weight fraction is not linear with temperature, as depicted in Fig. 5. A fit with a polynomial cubic function (but an exponential growth function also produced identical results) allowed to extract a firing temperature for the industrial bricks. The values, 980 °C and 992 °C, for SEB and STB samples, respectively, are about 15 °C higher than those obtained using the hematite content. However, in the range of temperatures of interest, the curves are flattening, decreasing the accuracy in the determination of the firing temperature. Because of the higher content in illite/smectite in the samples ST, also the weight fraction of mullite increases sensibly with dwell time (Table 3). Therefore, if the calibration curve is based on samples fired for longer times, the derived firing temperatures will be lower.

The Mg-spinel, which is between the products of decomposition of muscovite high in Fe (Grapes, 1986), as well as illite and kaolinite (McConville and Lee, 2005), is much less abundant than mullite in the studied samples, coherently with a relatively low Mg content and the modest amount of clinochlore in the raw clays.

In fact, experimental evidences link crystallization of spinel to clinochlore decomposition (Khalfaoui et al., 2006; Khalfaoui and Hajjaji, 2009). Other crystal-chemical aspects, such as the presence of alumina in the brucitic layer of chlorite (Khalfaoui and Hajjaji, 2009) or Mg substituting for Al in the illite lattice (McConville and Lee, 2005) may also play a role in favoring its crystallization. The formed spinel is high in Fe (McConville and Lee, 2005), and the incorporation of increasing amounts of foreign elements, increasing annealing time and/or temperature, has been considered the main reason for the observed increase in its unit-cell parameter a (Khalfaoui and Hajjaji, 2009). When the spinel weight fraction is considered, the results of the present investigation do not show any clear trend. Conversely, the unit-cell parameter a, obtained from the Rietveld refinements, increases with firing temperatures above 1000 °C (Fig. 6). Therefore, the plots are of no use for the assessment of firing conditions in the range of temperatures of interest. In case of sample ST the variation is negligible in the interval 900–1000 °C, whereas no spinel is present in the sample SE at 900 and 950 °C. The value of a (8.021 Å) obtained for sample STB is only indicating an upper limit for the firing temperature at 1000 °C.

Increasing dwell time at 950 °C had no effect on the unit-cell parameter, indicating that the kinetics of the site substitution in the crystal structure of spinel are fast enough to attain equilibrium (Parisi et al., 2014), as previously conjectured (Viani et al., 2016). On the other hand, the observed differences between the two classes of samples SE and ST, suggest that bulk chemical composition depends not only from maximum temperature (Principalle et al., 1989), but other physical-chemical aspects, connected with decomposition reactions and the mineralogical assemblage, might also play a role. However, some of the results graphically summarized in Fig. 6, still do not find a clear explanation. The unit-cell values measured at 1000 °C and 1050 °C in samples SE are higher with respect to the corresponding for samples ST, but in the former case, the products of decomposition of phyllosilicates

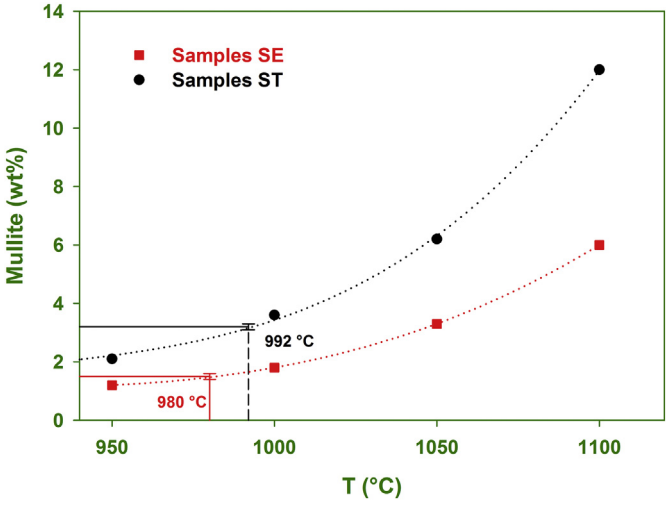

Fig. 5. Plot of mullite content vs. temperature with regression curves through the points for SE and ST samples fired in laboratory. Temperatures corresponding to bricks of industrial production are indicated. Where not indicated, error bars are within symbols.

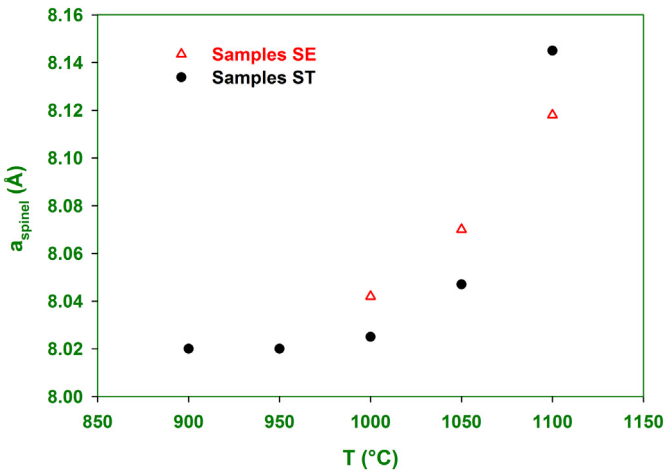

Fig. 6. Plot of unit-cell parameter a of spinel vs. MIP porosity for the indicated samples. Regression line through the points is reported. Error bars within symbols.

and illite/muscovite are lower, as it can be deduced from Table 2. At 1100 °C this trend is inverted, as it should be expected. Partial tentative explanation may come by considering that, for most of the investigated samples, the amount of spinel is low (< 2.5 wt%), which negatively affected the accuracy in the determination of the unit-cell parameter. This error is not reflected in the standard deviation obtained from the refinement, but is rather due to the difficulties in treating correctly the diffraction peaks of low intensity, due to partial overlap with those of other phases in the system. The observed differences could be also ascribed to the complex geochemical equilibria linked to the sequence of high-temperature transformations controlling the partitioning of foreign ions in the crystal structure of spinel.

A further component derived from the Rietveld refinement is the amount of amorphous fraction. It develops mostly as metastable product of decomposition of clay minerals below approximately 900 °C, but at higher temperatures it turns into a high-viscous alkaline glass. Unlike sintered ceramics, in which the amorphous is more uniformly distributed and mainly consisting of a glassy phase, in fired-clay bricks its nature is different and its development much more irregular (Khalfaoui and Hajjaji, 2009), reflecting the heterogeneous distribution of phyllosilicates within the matrix (Bauluz et al., 2004). From these considerations it follows that the relationship between amorphous fraction and firing temperature strongly depends upon the raw clay (Freyburg and Schwarz, 2007) and especially from the nature and amount of phyllosilicates.

Fig. 7, depicting the behavior of the amorphous content in the samples fired in the laboratory, confirms this view. A discontinuity is apparent at 900 °C. Above 900 °C, a smooth trend can be recognised, and has been described by curves representing an exponential function rising to a maximum. The two curves are displaced vertically, owing to the fact that samples ST, obtained from a raw material richer in clay minerals, develop more amorphous at every temperature. The firing temperatures obtained for the samples SEB and STB by plotting their amorphous content on the graph were 967 °C and 998 °C, respectively. The value for SEB is exactly the same obtained using the calibration curve for hematite, whereas a temperature 18 °C higher is derived from the sample STB.

The increase in dwell time to 5 h resulted in the increase of the weight fraction of amorphous phase in both samples, but at 7 h and 12 h a decrease was observed. Therefore, again the question is open on which conditions match closely those of the industrial cycle. This point is especially relevant for historical materials, where information on

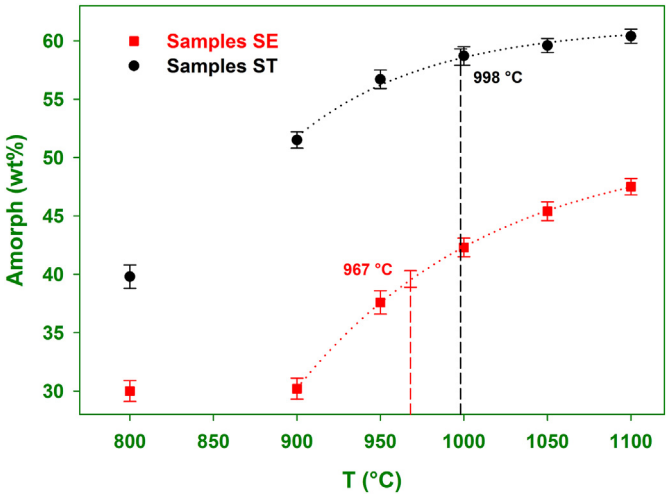

Fig. 7. Plot of amorphous content vs. temperature with regression curves through the points for SE and ST samples fired in laboratory. Temperatures corresponding to bricks of industrial production are indicated. Error bars within symbols.

production plants is often scarce. It can be supposed that, since dwell times of several hours are employed in the industrial cycle, longer dwell times (> 5 h) should be advisable for laboratory tests. However, it is the 'effective' temperature experienced by the fired body which matters, and, between other factors, this depends on sample size and volume of fired material with respect to the volume of the heating chamber. Moreover, temperature gradients inside the kiln might play a role. These aspects are still not well studied and there is no agreement in the literature on how to deal with such issues in case of fired-clay bricks (Freyburg and Schwarz, 2007; Khalfaoui et al., 2006; Khalfaoui and Hajjaji, 2009; McConville and Lee, 2005), or for the assessment of firing conditions of historical/archaeological fired bodies (Barone et al., 2011; Cultrone et al., 2005; De Rosa and Cultrone, 2014; Matsunaga and Nakai, 2004).

Adopting a more traditional approach, taking into account global QPA results, the mineral association and the microstructural data, a range of firing temperatures can also be inferred. In the present case, both SEB and STB samples show textural characteristics of the partially decomposed phyllosilicates similar to what reported for raw clays fired at temperatures between 900 and 1050 °C (Cultrone et al., 2001; Gualtieri, 2007; Iqbal and Lee, 2000). The microstructural and mineralogical changes in the fired body (Cultrone et al., 2004; Rodriguez-Navarro et al., 2003) with the dehydroxylation of phyllosilicates, the increase in the degree of sintering and the development of the amorphous fraction, bring about a decrease in porosity above 850–900 °C and a drop at 1100 °C (Freyburg and Schwarz, 2007), as evidenced in Table 1. At the same time, the pore-size distribution changes (Cultrone et al., 2004; Jordan et al., 2008), that is, the maximum in the distribution shift towards larger pores because of the disappearance of small pores and formation of larger ones (> 2 μm) (Delbrouck et al., 1993; Elert et al., 2003; Freyburg and Schwarz, 2007), which is graphically illustrated in Fig. 3. In this temperature interval also the relative fraction of open and closed pores changes, with an increase in closed porosity (not detected by MIP). The same processes have been observed also during sintering of ceramics (Kingery and Francis, 1965). However, it is worth noting that the microstructural parameters retrieved from MIP may lead to wrong conclusions. For the SEB sample, density and MIP porosity pointed to an inconsistently low firing temperature (around 800 °C), likely because of the difference between the industrial forming process and the one reproduced in the laboratory. This has been confirmed by the lower connectivity between grains observed with microscopy in the production brick. A similar discrepancy was not observed in the sample STB, because dried bodies from the production cycle were employed in the laboratory tests. Of the other methods for the characterization of brick samples, flexural strength is also not reliable for inferring the firing temperature of old bricks, because it suffers from high dispersion of the data, due to several aspects, such as the different manufacturing processes, inadequate quality control and deterioration effects (Cultrone et al., 2005; Grimm, 1988; Hansen and Kung, 1988; Lourenço et al., 2014).

The extracted values of firing temperature obtained from the three indicators considered in this work: hematite, mullite and amorphous phase, differed by < 20 °C, and reasonably matched the available information on the two industrial cycles. Essential to the obtainment of this result was, on one hand, the application of the Rietveld method with the addition of internal standard, which allows for the quantification of the amorphous/poorly crystalline fraction, and, on the other, the availability of the original raw clay. The latter is a critical aspect when dealing with historical or archaeological fired-clay materials. However, all proposed methods for the characterization of the production process, rely on the information on the raw material (see for example: (Barone et al., 2011; Hays et al., 2016; Maniatis and Tite, 1981; Matsunaga and Nakai, 2004)). The reported examples clearly lack of statistical significance, which is also frequently the case for historical or archaeological objects. This issue should not be of major concern when dealing with not deteriorated production bricks, because

each step of the production process (e.g. homogenization of the raw clay, size reduction, drying and firing time and temperature) is optimized to ensure constant properties of the fired body. As pointed out above, the proposed approach can be applied only when one has knowledge on the forming process and has access to the original raw clay. Undoubtedly, further experimental work is needed in order to better understand the parameters affecting the 'effective' temperature experienced by the fired body for its applicability to other clay-based materials.

5. Conclusions

Between the conservative actions aimed at the preservation of objects part of cultural heritage, brick replacement occurs frequently, and often involves the production of new bricks. As a widely accepted principle, the characteristics of existing and replacement bricks should match. Therefore, ideal conditions for the production of custom made replacement bricks are the availability of the original raw materials and the knowledge of the thermal cycle. In this work we have proposed an approach to the assessment of maximum firing temperature making use of calibration curves built up from the results of QPA and the Rietveld method. This approach has been tested on two masonry bricks fired in the industrial cycle, using calibration curves for hematite, mullite and the amorphous fraction, and built using the original raw clays fired in laboratory at different temperatures. The values obtained from the three curves differed for < 20 °C and reasonably matched the nominal temperatures of the industrial cycles. A dependence of mineralogical composition of the fired-clays from dwell time between 3 h and 12 h at 950 °C, has been observed. The raw clay with high content in illite/muscovite (38.1 wt%) showed the highest variations because of the role played by its thermal decomposition. At present, no simple solution to deal with this issue, which is a downside of the proposed method, is available. This subject will be matter of further studies. Applicability of the method is limited to cases in which both the original raw clay and information on the forming process are available.

Declarations of interest

None.

Acknowledgements

This research was supported by the project No. LO1219 under the Ministry of Education, Youth and Sports of Czech Republic and the research project MAT2016-75889-R of the Spanish Ministry of Economy and Competitiveness. The authors would like to thank Ing. Milan Svoboda (MIP analysis), Eva Pažourková (preparation of thin and polished sections), Roman Fabeš (sample preparation), and Jaroslav Buzek (information about the brickyard in Sedlejov) from the Centre of Excellence Telč. Martin Vyšvařil from Brno University of Technology for the X-ray fluorescence analysis, and Cihelna Štěrboholy for having provided samples and information about the brickyard.

Appendix A. Supplementary data

Supplementary data to this article can be found online at https://doi.org/10.1016/j.clay.2018.07.020.

References

Akinshipe, O., Kornelius, G., 2017. Chemical and thermodynamic processes in clay brick firing technologies and associated atmospheric emissions metrics-a review. J. Pollut. Eff. Control 5. https://doi.org/10.4172/2375-4397.1000190.

Alonso-Santurde, R., Andrés, A., Viguri, J.R., Raimondo, M., Guarini, G., Zanelli, C., Dondi, M., 2011. Technological behaviour and recycling potential of spent foundry sands in clay bricks. J. Environ. Manag. 92, 994–1002. https://doi.org/10.1016/j.jenvman.2010.11.004.

Baer, N., Livingstone, F., 2015. Conservation of Historic Brick Structures. Routledge, New York.

Ballato, P., Cruciani, G., Dalconi, M.C., Fabbri, B., Macchiarola, M., 2005. Mineralogical study of historical bricks from the great palace of the byzantine emperors in Istanbul based on powder X-ray diffraction data. Eur. J. Mineral. 17, 777–784. https://doi.org/10.1127/0935-1221/2005/0017-0777.

Barlow, S.G., Manning, D. a C., Hill, P.I., 1997. Influence of time and temperature on reactions and transformations of clinochlore as a ceramic clay mineral. Br. Ceram. Trans. 96, 195–198.

Barone, G., Crupi, V., Majolino, D., Mazzoleni, P., Teixeira, J., Venuti, V., Scandurra, A., 2011. Small angle neutron scattering as fingerprinting of ancient potteries from Sicily (Southern Italy). Appl. Clay Sci. 54, 40–46. https://doi.org/10.1016/j.clay.2011.07.010.

Bauluz, B., Mayayo, M.J., Yuste, A., Fernandez-Nieto, C., Gonzalez Lopez, J.M., 2004. TEM study of mineral transformations in fired carbonated clays: relevance to brick making. Clay Miner. 39, 333–344. https://doi.org/10.1180/0009855043930138.

ČGS, 2018. Geological Map of Czech Republic 1:50,000 [WWW Document]. http://www.geology.cz/extranet-eng/maps/online/map-applications, Accessed date: 4 February 2018.

Chlupáč, J., Brzobohatý, R., Kovanda, J., Stráník, Z., 2002. Geologická minulost České republiky. Academia, Prague.

Cline, J.P., Von Dreele, R.B., Winburn, R., Stephens, P.W., Filliben, J.J., 2011. Addressing the amorphous content issue in quantitative phase analysis: the certification of NIST standard reference material 676a. Acta Crystallogr. Sect. A Found. Crystallogr. 67, 357–367. https://doi.org/10.1107/S0108767311014565.

Cultrone, G., Rodriguez-Navarro, C., Sebastian, E., Cazalla, O., De La Torre, M.J., 2001. Carbonate and silicate phase reactions during ceramic firing. Eur. J. Mineral. 13, 621–634. https://doi.org/10.1127/0935-1221/2001/0013-0621.

Cultrone, G., Sebastián, E., Elert, K., de la Torre, M.J., Cazalla, O., Rodriguez-Navarro, C., 2004. Influence of mineralogy and firing temperature on the porosity of bricks. J. Eur. Ceram. Soc. 24, 547–564. https://doi.org/10.1016/S0955-2219(03)00249-8.

Cultrone, G., Sidraba, I., Sebastián, E., 2005. Mineralogical and physical characterization of the bricks used in the construction of the "Triangul Bastion", Riga (Latvia). Appl. Clay Sci. 28, 297–308. https://doi.org/10.1016/j.clay.2004.02.005.

de Bakker, P.M.A., De Grave, E., Vandenberghe, R.E., Bowen, L.H., Pollard, R.J., Persoons, R.M., 1991. Mössbauer study of the thermal decomposition of lepidocrocite and characterization of the decomposition products. Phys. Chem. Miner. 18, 131–143. https://doi.org/10.1007/BF00216606.

De Bonis, A., Cultrone, G., Grifa, C., Langella, A., Leone, A.P., Mercurio, M., Morra, V., 2017. Different shades of red: the complexity of mineralogical and physico-chemical factors influencing the colour of ceramics. Ceram. Int. 43, 8065–8074. https://doi.org/10.1016/j.ceramint.2017.03.127.

De Rosa, B., Cultrone, G., 2014. Assessment of two clayey materials from northwest Sardinia (Alghero district, Italy) with a view to their extraction and use in traditional brick production. Appl. Clay Sci. 88–89, 100–110. https://doi.org/10.1016/j.clay.2013.11.030.

Delbrouck, O., Janssen, J., Ottenburgs, R., Van Oyen, P., Viaene, W., 1993. Evolution of Porosity in Extruded Stoneware as a Function of Firing Temperature. vol. 8. pp. 187–192.

Dondi, M., Mazzanti, F., Principi, P., Raimondo, M., Zanarini, G., 2004. Thermal conductivity of clay bricks. J. Mater. Civ. Eng. 16, 8–14. https://doi.org/10.1061/(ASCE)0899-1561(2004)16:1(8).

Elert, K., Cultrone, G., Navarro, C.R., Pardo, E.S., 2003. Durability of bricks used in the conservation of historic buildings — influence of composition and microstructure. J. Cult. Herit. 4, 91–99. https://doi.org/10.1016/S1296-2074(03)00020-7.

Freyburg, S., Schwarz, A., 2007. Influence of the clay type on the pore structure of structural ceramics. J. Eur. Ceram. Soc. 27, 1727–1733. https://doi.org/10.1016/j.jeurceramsoc.2006.04.158.

Grapes, R.H., 1986. Melting and thermal reconstitution of pelitic xenoliths, wehr volcano, east eifel, West Germany. J. Petrol. 27, 343–396. https://doi.org/10.1093/petrology/27.2.343.

Grimm, C.T., 1988. Masonry cracks: a review of the literature. In: Harris, H. (Ed.), Masonry: Materials, Deasign, Construction, and Maintenance. ASTM International, 100 Barr Harbor Drive, PO Box C700, West Conshohocken, PA 19428-2959, pp. 257–280.

Gualtieri, A.F., 2007. Thermal behavior of the raw materials forming porcelain stoneware mixtures by combined optical and in situ X-ray dilatometry. J. Am. Ceram. Soc. 90, 1222–1231. https://doi.org/10.1111/j.1551-2916.2007.01614.x.

Gualtieri, A.F., Brignoli, G., 2004. Rapid and accurate quantitative phase analysis using a fast detector. J. Appl. Crystallogr. 37, 8–13. https://doi.org/10.1107/S0021889803022052.

Gualtieri, A.F., Guagliardi, A., Iseppi, A., 2004. The quantitative determination of the crystalline and the amorphous content by the Rietveld method: application to glass ceramics with different absorption coefficients. pp. 147–165. https://doi.org/10.1007/978-3-662-06723-9_6.

Gualtieri, M.L., Gualtieri, A.F., Gagliardi, S., Ruffini, P., Ferrari, R., Hanuskova, M., 2010. Thermal conductivity of fired clays: effects of mineralogical and physical properties of the raw materials. Appl. Clay Sci. 49, 269–275. https://doi.org/10.1016/j.clay.2010.06.002.

Gualtieri, A.F., Riva, V., Bresciani, A., Maretti, S., Tamburini, M., Viani, A., 2014. Accuracy in quantitative phase analysis of mixtures with large amorphous contents. The case of stoneware ceramics and bricks. J. Appl. Crystallogr. 47, 835–846. https://doi.org/10.1107/S160057671400627X.

Hansen, W., Kung, J.H., 1988. Pore structure and frost durability of clay bricks. Mater. Struct. 21, 443–447. https://doi.org/10.1007/BF02472325.

Hays, C.T., Weinstein, R.A., Stoltman, J.B., 2016. Poverty point objects reconsidered.

Southeast. Archaeol. 35, 213–236. https://doi.org/10.1080/0734578X.2016.1165050.
Iqbal, Y., Lee, W.E., 2000. Microstructural Evolution in Triaxial Porcelain. J. Am. Ceram. Soc. 83, 3121–3127. https://doi.org/10.1111/j.1151-2916.2000.tb01692.x.
Jordan, M.M., Montero, M.A., Meseguer, S., Sanfeliu, T., 2008. Influence of firing temperature and mineralogical composition on bending strength and porosity of ceramic tile bodies. Appl. Clay Sci. 42, 266–271. https://doi.org/10.1016/j.clay.2008.01.005.
Khalfaoui, A., Hajjaji, M., 2009. A Chloritic-illitic clay from Morocco: temperature–-time–transformation and neoformation. Appl. Clay Sci. 45, 83–89. https://doi.org/10.1016/j.clay.2009.03.006.
Khalfaoui, A., Kacim, S., Hajjaji, M., 2006. Sintering mechanism and ceramic phases of an illitic–chloritic raw clay. J. Eur. Ceram. Soc. 26, 161–167. https://doi.org/10.1016/j.jeurceramsoc.2004.10.030.
Kingery, W.D., Francis, B., 1965. Grain growth in porous compacts. J. Am. Ceram. Soc. 48, 546–547. https://doi.org/10.1111/j.1151-2916.1965.tb14665.x.
Kovanda, J., Balatka, B., Bernard, J., Brunnerová, Z., Březinová, D., Bukanovská, M., Cílek, V., 2001. Neživá příroda Prahy a jejího okolí. Acaremia, Prague.
Laita, E., Bauluz, B., 2018. Mineral and textural transformations in aluminium-rich clays during ceramic firing. Appl. Clay Sci. 152, 284–294. https://doi.org/10.1016/j.clay.2017.11.025.
Lourenço, P.B., Van Hees, R., Fernandes, F., Lubelli, B., 2014. Characterization and damage of brick masonry. In: Structural Rehabilitation of Old Buildings, pp. 109–130. https://doi.org/10.1007/978-3-642-39686-1.
Luna, J., 2005. Geologická stavba, těžba nerostných surovin, mineralogické poměry. In: Dačicko, Slavonicko, Telčsko, Moravská, Vlastivěda (Eds.), Muzejní a vlastivědná společnost v Brně, Brno, pp. 11–26.
Maniatis, Y., Tite, M.S., 1981. Technological examination of Neolithic-Bronze Age pottery from central and southeast Europe and from the Near East. J. Archaeol. Sci. 8, 59–76. https://doi.org/10.1016/0305-4403(81)90012-1.
Maniatis, Y., Simopoulos, A., Kostikas, A., 1981. Moessbauer study of the effect of calcium content on iron oxide transformations in fired clays. J. Am. Ceram. Soc. 64, 263–269. https://doi.org/10.1111/j.1151-2916.1981.tb09599.x.
Matsunaga, M., Nakai, I., 2004. A study of the firing technique of pottery from Kaman-Kalehoyuk, Turkey, by synchrotron radiation-induced fluorescence X-ray absorption near-edge structure (Xanes) analysis*. Archaeometry 46, 103–114. https://doi.org/10.1111/j.1475-4754.2004.00146.x.
McConville, C.J., Lee, W.E., 2005. Microstructural development on firing illite and smectite clays compared with that in kaolinite. J. Am. Ceram. Soc. 88, 2267–2276. https://doi.org/10.1111/j.1551-2916.2005.00390.x.
Parisi, F., Lenaz, D., Princivalle, F., Sciascia, L., 2014. Ordering kinetics in synthetic Mg $(Al,Fe^{3+})_2O_4$ spinels: quantitative elucidation of the whole Al-Mg-Fe partitioning, rate constants, activation energies. Am. Mineral. 99, 2203–2210. https://doi.org/10.2138/am-2014-4853.
Podoba, R., Kaljuvee, T., Štubňa, I., Podobník, Ľ., Bačík, P., 2014. Research on historical bricks from a Baroque Church. J. Therm. Anal. Calorim. 118, 591–595. https://doi.org/10.1007/s10973-013-3417-4.
Princivalle, F., Della Giusta, A., Carbonin, S., 1989. Comparative crystal chemistry of spinels from some suites of ultramafic rocks. Miner. Pet. 40, 117–126.
Rodriguez-Navarro, C., Cultrone, G., Sanchez-Navas, A., Sebastian, E., 2003. TEM study of mullite growth after muscovite breakdown. Am. Mineral. 88, 713–724. https://doi.org/10.2138/am-2003-5-601.
de Rojas, M.I.S., Azorín, V., Frías, M., Rivera, J., García, N., Martin-Estarlich, A., Saiz-Jimenez, C., 2004. Weathering, cleaning and conservation of the brick façade on the "Niño Jesus" Hospital in Madrid, in: Saiz-Jimenez, C. (Ed.), Air Pollution and Cultural Heritage: Proceedings of the International Workshop, Seville, December 1–3, 2003. Taylor & Francis Group, London, pp. 233–238.
Schiavon, N., Mazzocchin, G.A., Baudo, F., 2008. Chemical and mineralogical characterisation of weathered historical bricks from the Venice lagoonal environment. Environ. Geol. 56, 767–775. https://doi.org/10.1007/s00254-008-1481-z.
Scolforo, M., Browne, H., 1996. Acquisition and properties of brick for historic structure preservation and rehabilitation. In: Standards for Preservation and Rehabilitation. ASTM International, 100 Barr Harbor Drive, PO Box C700, West Conshohocken, PA 19428-2959, pp. 337–347. https://doi.org/10.1520/STP15447S.
Slavík, J., Smutný, J., Tothová, J., Horváthová, Konůpková, Jana Konůpek, J., Albrecht, P., Hudák, L., Papoušek, M., Kibic, K., Vašata, M., Řehák, J., Wohlmuth, P., 2014. Bastionové pevnosti: průzkumy a opravy. Národní památkový ústav, Ústí nad Labem, Czechia.
Valanciene, V., Siauciunas, R., Baltusnikaite, J., 2010. The influence of mineralogical composition on the colour of clay body. J. Eur. Ceram. Soc. 30, 1609–1617. https://doi.org/10.1016/j.jeurceramsoc.2010.01.017.
Válek, J., van Halem, E., Viani, A., Pérez-Estébanez, M., Ševčík, R., Šašek, P., 2014. Determination of optimal burning temperature ranges for production of natural hydraulic limes. Constr. Build. Mater. 66, 771–780. https://doi.org/10.1016/j.conbuildmat.2014.06.015.
Viani, A., Sotiriadis, K., Len, A., Šašek, P., Ševčík, R., 2016. Assessment of firing conditions in old fired-clay bricks: the contribution of X-ray powder diffraction with the Rietveld method and small angle neutron scattering. Mater. Charact. 116, 33–43. https://doi.org/10.1016/j.matchar.2016.04.003.
Young, R., 1993. The Rietveld Method, by RA Young. Oxford University Press, Oxford. https://doi.org/10.1017/CBO9781107415324.004.